Design and Modeling of Membrane Supported FBAR Filter

Alexandra STEFANESCU, Dan NECULOIU, Alina Cristina BUNEA

IMT Bucharest, 32B, Erou Iancu Nicolae str., 077190 Bucharest, Romania
Tel.: +40212690775

Abstract. This paper introduces a novel technique for the electromagnetic modeling of the Film bulk acoustic resonator (FBAR) filters. The piezoelectric equations are coupled to the Maxwell's equations through a Lorentz dispersive model. First, FEM (Finite Element Method) simulations are performed for an FBAR resonator in order to observe the resonant behaviour of the device. Then, the Lorentz model is extracted from the FEM results and is introduced in the electromagnetic (EM) design of the FBAR filter.

1. Introduction

With the development of mobile and satellite communication as well as data transmission (WLAN), film bulk acoustic resonators (FBAR) have attracted a major interest in the fabrication of radio frequency (RF) filters. These applications need small size, high quality factors and monolithic integration with active electronic devices. FBAR devices have the potential advantages to act as key components for wireless communication and sensing network systems [1], [2].

The most common wide band gap (WBG) materials are SiC, GaN and AlN, the last two with pronounced piezoelectric properties. The sub-micron thickness of the GaN or AlN membrane in FBAR devices will result in an operating frequency up to 6 GHz and above. Recently the first FBAR structures manufactured on GaN membranes have been reported [3], [4].

Most of the designs presented thus far are based on equivalent circuits - 1D Mason's model [5, 6] or distributed models based on Krimtholz, Leedom and Matthaei circuit (KLM) [7]. Since one of the main challenges in designing FBAR structures is to avoid the unwanted resonances, different numerical techniques have been used in literature, most of them based on Finite Element Method (FEM) [8, 9]. All these methods analyze the FBAR structure from the mechanical and electrical point of view. The relative high frequencies and the metallization thickness

comparable with the piezoelectric membrane thickness impose the development of an advanced modeling technique.

This paper proposes a novel method for design and modeling of the FBAR filters (Fig. 1). The method consists in linking the FEM piezoelectric simulations for a simple configuration of FBAR composed of metal/piezoelectric-film/metal layers with symmetric top and bottom electrodes with the electromagnetic design of a complete three resonator band-pass filter by including a Lorentz dispersive model for the piezoelectric material in CST Microwave Studio. This method permits a complete 3D detailed modeling that also analyzes the microwave behaviour of the FBAR filter.

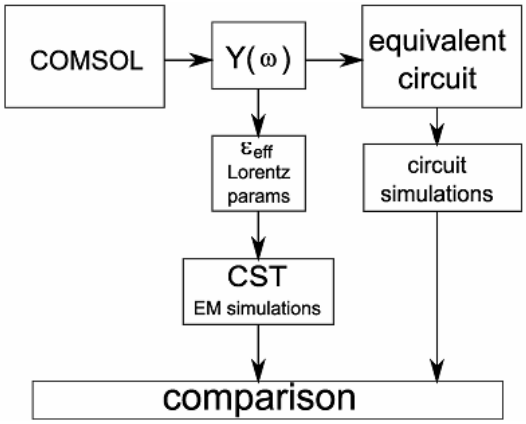

Fig. 1. Flow chart of the modeling technique.

A coupled analysis of the EM modeling with the solution of the acoustic equations for the Thin Film Bulk Acoustic Resonators has been developed by Farina and Rozzi in [10].

The paper is organized as follows. Section 2 presents the modeling of the FBAR resonators used in the filter design and Section 3 describes the electromagnetic simulation results obtained with CST Microwave Studio for the FBAR filter. Finally, we conclude and propose future paths of research in Section 4.

2. Fem Simulation

Simulations with Finite Element Method (FEM) software, COMSOL [11] were carried out to investigate the frequency response analysis for two BAW resonators. In both cases, the lowest layer is Molybdenum (50 nm thick) that operates as ground electrode. Next, the buffer layer (composed from AlGaN) is 0.3 μm thick and the GaN undoped layer has also 0.3 μm. On top of the resonator there is another Molybdenum electrode: resonator A – 50 nm thick and 100 μm wide – and resonator B – 50 nm thick and 150 μm wide. The relation between the strain,

electric field and electric displacement field in a strain-charge form is given by the piezoelectric constitutive equations (1) and (2):

$$S = s_E T + d^T E \tag{1}$$

$$D = dT + \varepsilon_T E \tag{2}$$

where **S** represents the strain matrix, **T** is the stress matrix, **E** is the electric field applied to the resonator, D is the electric density displacement matrix, d, s_E, and ε_T are piezoelectric material constants. The piezoelectric strain constants, permittivity and density are taken from [12]. The model geometry (Fig. 2) is a symmetric section in the centre of the layout. For the frequency analysis the geometry was extended with perfectly matched layer (PML) domains at the membrane edges, in order to increase the length of the resonator. These layers have the property of absorbing the energy of the acoustic waves that cross the exterior boundaries of the model.

The boundary conditions are set as follows: the bottom electrode (grounded, V_0=0) is fixed, and an electric potential is applied on the top electrode (V_0=1). The rest of the boundaries are free zero charge, excepting the truncation boundaries which are fixed.

In the frequency response analysis the admittance of the resonator is estimated with (3):

$$Y(\omega) = \frac{J_{ns}}{V_0} \tag{3}$$

where J_{ns} is the current through the top electrode and ω is the angular frequency.

The geometry of resonator A is presented in Fig. 2. The insets represent the electric potential variations for the resonant and antiresonant frequencies.

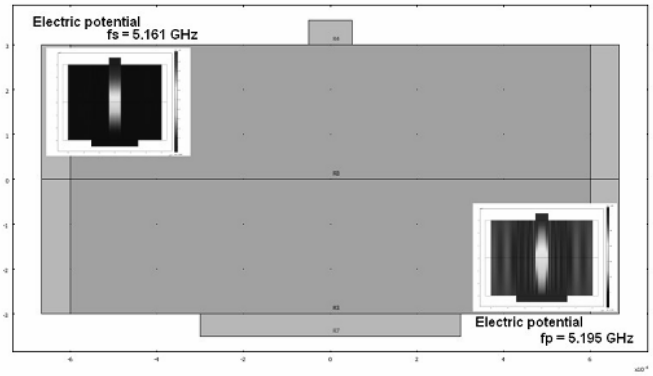

Fig. 2. FEM model for FBAR (inset – simulation results for resonator A).

Figure 3 shows the graph of the admittance as a function of frequency. For both resonators a series resonant frequency at 5.161 GHz and one parallel resonant frequency at 5.195 GHz have been obtained. As expected, an increase in the static capacitance is observed with the increase of the top electrode area.

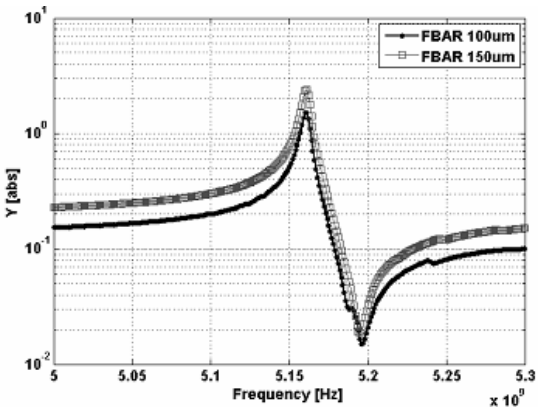

Fig. 3. Compared simulated electrical admittance versus frequency for the two FBAR structures.

The equivalent Butterworth – Van – Dyke circuit representation [1, 13] is used in the resonators modeling process (Fig. 4) in order to extract the optimum areas for the electrodes by fitting the results obtained with COMSOL:

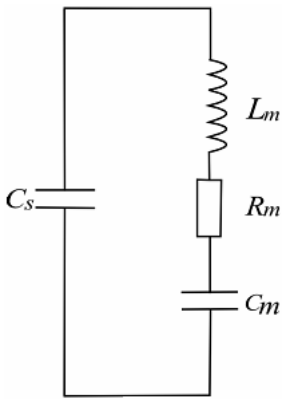

Fig. 4. Butterworth – Van – Dyke equivalent circuit of the FBAR resonator.

The circuit includes a static capacitance, C_s and a motional arm having a dynamic inductor L_m, a dynamic capacitance C_m and a dynamic loss R_m.

The values extracted from the equivalent circuit for the two resonators are depicted in Table 1.

Table 1. Characteristics of each FBAR used in designing the FBAR filter

FBAR component	FBAR A	FBAR B
Area Size [μm^2]	100 μm × 300 μm	150 μm × 300 μm
C_s [pF]	0.225	0.222
C_m [pF]	18.2	18.8
R_m [Ω]	0.5	0.48
Lm [nH]	4.136	2.152

The structure is similar to a parallel plate capacitor which allows the evaluation of the permittivity of the dielectric material, ε [12] with (4):

$$\varepsilon(\omega)=\frac{|Y(\omega)|}{\omega\frac{A}{t}}, \tag{4}$$

where A represents the electrodes area and t is the thickness of the dielectric layer (GaN).

3. Electromagnetic Simulation and Modeling

The FBAR filter has a standard pass band configuration, containing two series connected resonators (A) and a parallel one (B). The performance of the filter is dictated by the individual performances of the resonators [14].

The FBAR filter topology is represented in Fig. 5. This configuration was chosen due to the backside metallization of the membrane that has the key role of an electrode with floating potential. The access electrodes are defined on the front side.

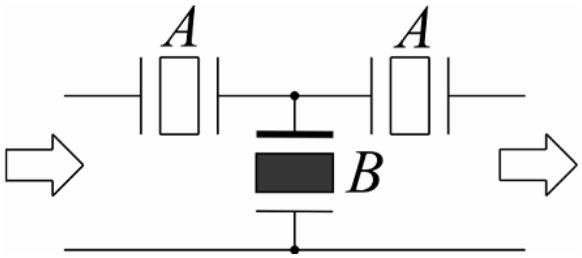

Fig. 5. FBAR Filter topology

A 3D view of the structure is shown in Fig. 6. The two lateral resonators have a width of 100 μm and a length of 300 μm, while the central one has a width of 150 μm and the same length.

The filter is fed by means of 50/100/50 μm coplanar waveguide transmission lines.

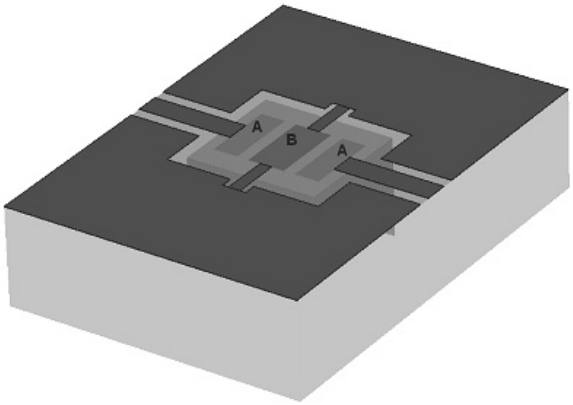

Fig. 6. EM model for FBAR.

The main dimensions of the layout are shown in Fig. 7. The inset presents a schematic cross section of the active part of the structure.

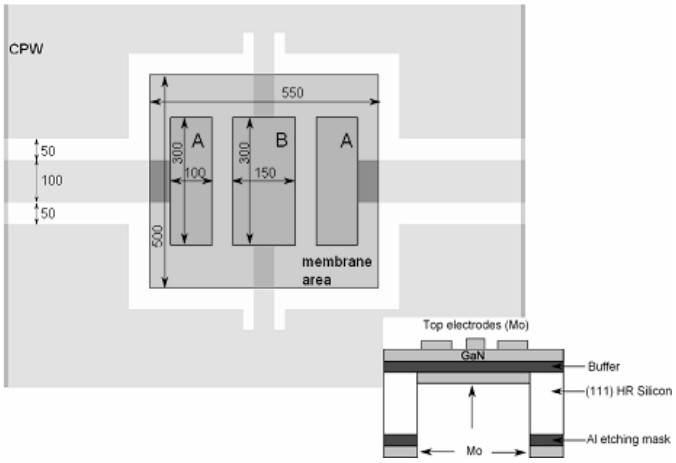

Fig. 7. Layout of the simulated structure (inset – cross section).

The above design is simulated with CST Microwave Studio (MWS) [15]. The port definition and S parameter extraction are optimized for electric field distribution (ideal for waveguide port and planar ports with multiple pins definition feature). For this structure, the Frequency Domain Solver has been used.

In order to solve the coupled piezoelectric/electromagnetic equations, we need to define a material dispersion curve for the electric permittivity so that the electrical displacement (5) used in the full-wave EM analysis

$$D = \varepsilon_T E \tag{5}$$

to comprise the piezoelectric effect. To catch the resonance behaviour of the piezoelectric material, the Lorentz model is applied for the electric permittivity (ε) obtained with (4):

$$\varepsilon_r(\omega) = \varepsilon_\infty + \frac{(\varepsilon_s - \varepsilon_\infty)\omega_0^2}{\omega_0^2 - \omega^2} \tag{5}$$

where ω_0 is the resonance frequency and ε_∞ is the relative permittivity of the Gallium Nitride material. The dielectric loss tangent (tanδ) of the piezoelectric film is not added in the model.

Figure 8 shows the real (ε') and imaginary parts (ε") of the relative permittivity extracted for resonator A, demonstrating the material resonance at the resonance frequency (Table 2).

Table 2. Material parameters used for Lorentz model

	FBAR A	**FBAR B**
ε_∞	9	9
ε_s	8.66	8.66
f resonance [Hz]	5.12e9	5.23e9
f damping [Hz]	22e7	26.6e7

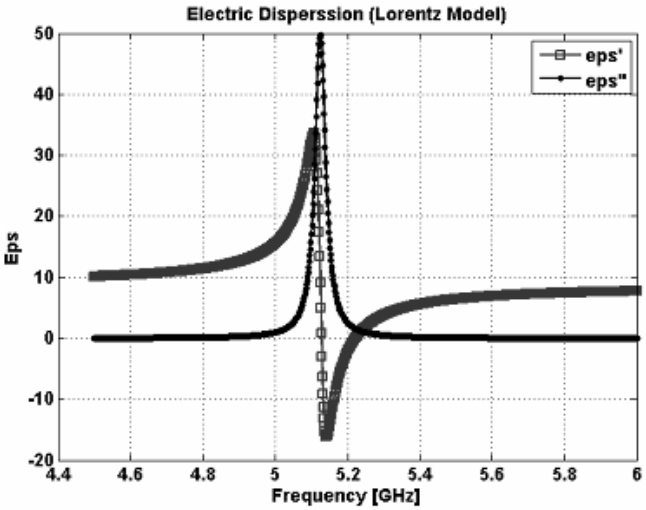

Fig. 8. Resonance behaviour of GaN extracted with Lorentz model for the electrodes type A.

The simulated transmission and reflection parameters are reported in Fig. 9. The filter is centered at 5.2 GHz.

Figure 10 shows the transmission parameter for the filter simulated with an electrical circuit software simulator.

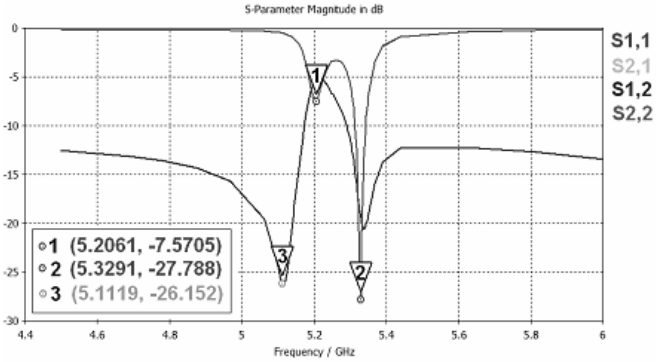

Fig. 9. FBAR filter characteristics. Transmission response S21 (dark) and reflection S11 (dashed).

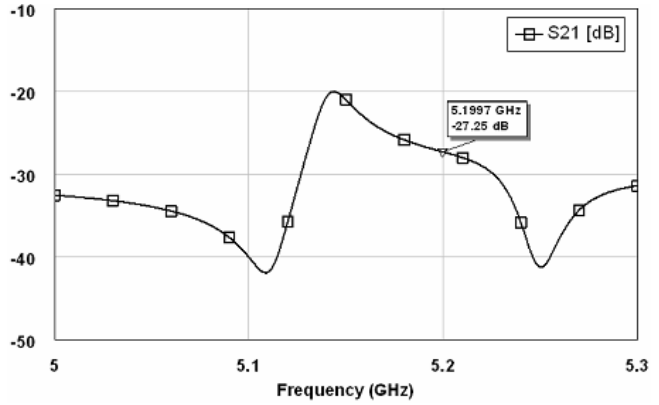

Fig. 10. Simulated transmission parameter for the FBAR filter structure.

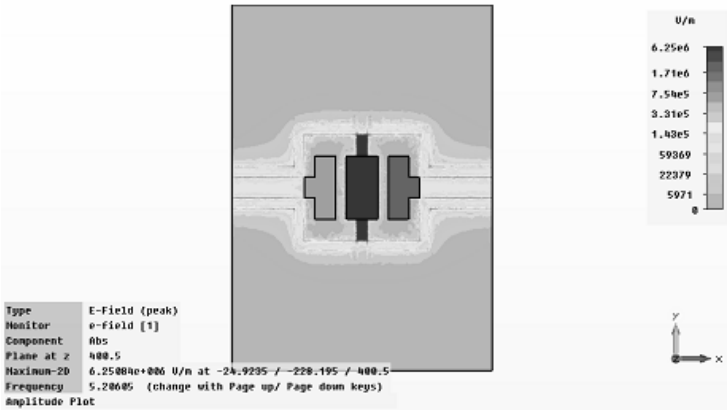

Fig. 11. Electric field distribution at 5.206 GHz.

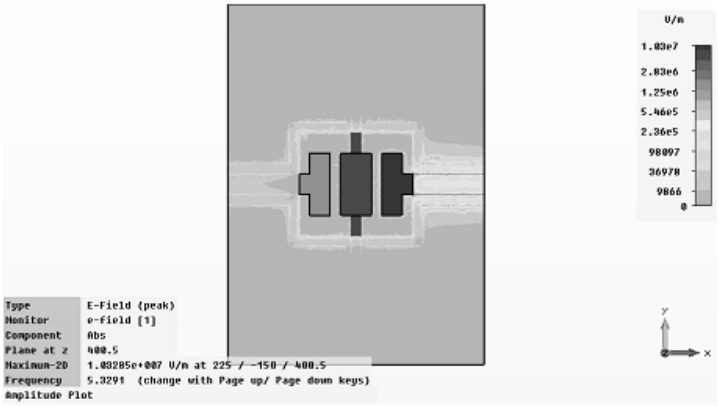

Fig. 12. Electric field distribution at 5.321 GHz.

Figures 11 and 12 show the electric field distribution in the xy plane at the frequencies marked with 1 (5.206 GHz) and 2 (5.321 GHz) in Fig. 9.

4. Conclusion

FEM and EM simulations have been carried out for the membrane supported FBAR filter. A novel modeling approach that links the piezoelectric simulation (COMSOL Multiphysics) of the device with the electromagnetic model (CST Microwave Studio) is presented. This work will be used for the design, characterization and parameter extraction of the membrane supported FBAR filter.

Acknowledgement. The author Alexandra Stefanescu acknowledges the support of the Sectoral Operational Program Human Resource Development (SOP HRD) financed from the European Social Fund and by the Romanian Government under the contract number POSDRU/89/1.5/S/63700.

References

[1] C.M. FANG, S.C. LIN, Y.C. CHIN, P.Y. CHEN, H.R. LIN, P.Z. CHANG, *5.4 GHz high-Q bandpass filter for wireless sensor network system*, Sensors, IEEE, 2009.

[2] H-W CHOI, J-Y. JUNG, S-K. LEE, Y-S. PARK, K-H. KIM, *The Designing of an Air-gap Type FBAR Filter using Leach Equivalent Model*, Transactions on Electrical and Electronic Materials, **7**(4), 2006.

[3] D. NECULOIU, G. KONSTANTINIDIS, A. MÜLLER, A. KOSTOPOULOS, D. VASILACHE, K.MUTAMBA, C. SYDLO, H. L. HARTNAGEL, L. BARY, R. PLANA, *Microwave FBAR Structures Fabricated using Micromachined GaN Membranes*, International Microwave Symposium Digest, IEEE MTT-S, pp. 877–880, 2007,.

[4] A. MÜLLER, D. NECULOIU, G. KONSTANTINIDIS, A. STAVRINIDIS, D. VASILACHE, A. CISMARU, M. DANILA, M. DRAGOMAN, G. DELIGEORGIS and K. TSAGARAKI, *6.3-GHz Film Bulk Acoustic Resonator Structures Based on a Gallium Nitride/Silicon Thin Membrane*, Electron Device Letters, IEEE, **30**(8), pp. 799–801, 2009.

[5] W. PANG, H. ZHANG, H. YU, E.S. KIM, *Analytical and Experimental Study on Second Harmonic Response of FBAR for Oscillator Applications above 2GHz*, Ultrasonics Symposium, IEEE, **4**, pp. 2136–2139, 2005.
[6] Y. ZHANG, Z. WANG, J. DAVID N. CHEEKE, *Resonant Spectrum Method to Characterize Piezoelectric Films in Composite Resonators*, IEEE Transactions on Ultrasonics, Ferroelectrics and Frequency Control, **50**(3), pp. 321–333, 2003.
[7] C. COLLADO, E. ROCAS, J. MATEU, A. PADILLA, J.M. O'CALLAGHAN, *Nonlinear Distributed Model for Bulk Acoustic Wave resonators*, IEEE Transactions on Microwave Theory and Techniques, **57**(12), 2009.
[8] H. CAMPANELLA, E. MARTINCIC, P. NOUET, A. URANGA, J. ESTEVE, *Analytical and Finite-Element Modeling of Localized-Mass Sensitivity of Thin-Film Bulk Acoustic-Wave Resonators (FBAR)*, IEEE Sensors Journal, **9**(8), pp. 892–901, 2009.
[9] J. VERDU, P. DE PACO, O MENDEZ, *Electric Equivalent Circuit for the Thickened Edge Load Solution in a Bulk Acoustic Wave Resonator*, Progress in Electromagnetic Research M, **11**, 2010.
[10] M. FARINA, T. ROZZI, *Electromagnetic Modeling of Thin Film Bulk Acoustic Resonators*, IEEE Transactions on Microwave Theory and Techniques, **25**(11), 2004.
[11] COMSOL webpage: www.comsol.com
[12] http://ioffe.ru
[13] H. CAMPANELLA, *Acoustic Wave and Electromechanical Resonators, Concept to Key Applications*, Artech House Integrated Microsystems Series, 2010.
[14] Tuomas PENSALA, *Thin Film Bulk Acoustic Wave Devices. Performance Optimization and Modeling*, VTT publication 756, phd Thesis, 2011
[15] CST webpage: www.cst.com